EFFECT OF DROPLET INJECTION ON PARTICLE SEPARATION EFFICIENCY OF CYCLONE SEPARATORS

A. Momenzadeh†, M. Moghiman††

†Department of Mechanical Engineering, Ferdowsi University of Mashhad, Mashhad, I. R. of Iran

Email: amirmomenzadeh@yahoo.com

††Department of Mechanical Engineering, Ferdowsi University of Mashhad, Mashhad, I. R. of Iran

Email: mmoghiman@yahoo.com

Abstract. *This paper presents the effect of liquid droplet injection on separation efficiency in a cyclone separator using a numerical procedure. As common cyclone separators (dry cyclone separators) unable to collect fine particles efficiently, the liquid droplets are injected into cyclone chamber, to improve separation efficiently of cyclone separators. The major focus is the study of the effect of liquid droplet injection, on the collection of particles with diameter smaller than 10 microns.*

The problem of isothermal flow-field in cyclone separators is formulated in terms of the Eulerian partial differential equations of the gas phase conservation of mass and momentum An algebraic Reynolds stress model (ASM), is also used to involve turbulence efefcts. A Lagrangian approach is employed to predict the trajectories of discrete phase (particles and droplets) in cyclone chamber. The effect of velocity fluctuations on separation efficiency is studied by use of instantaneous fluctuating velocities instead of the mean velocities.

The solid particles and liquid droplets are introduced in a converged flow solution. The injected droplets collect particles by use of one or more several collection mechanisms. In cyclone separators, Impaction is the principle collection mechanism. The detailed effects of droplet injector design parameters (such as nozzle angle, droplet velocity and droplet diameter) on the collection performance, are investigated.

The calculations show that a droplet trajectory is strongly influenced by droplet size. The simulation results also show that injection of liquid droplet can enhance separation efficiency of cyclone separator, especially for particles <5 μm. Numerical results also indicate that taking fluctuation velocities into account would decrease separation efficiency of cyclones. Comparisons between predicted results and measurements show good agreement.

Key words: cyclone separator, separation efficiency, droplet injection, Stokes number, impaction mechanism

1 INTRODUCTION

A cyclone separator is a static device that employs centrifugal force for the separation of the dense phase from a two-phase flow. Generally, the gas–solid mixture enters the cyclone separator, through the tangential inlet on the top section of main body. Then, the cylindrical wall makes a downward swirling motion. Centrifugal force moves the dusts toward the walls of the cylinder and down the conical section, to the dust outlet; the cleaned gas, finally, exits through the vortex finder.

Due to main advantages of cyclone separators including geometrical simplicity and low manufacturing, installation, operation and maintenance costs; cyclone separators are extensively used in various industries in the field of air pollution control and gas-solid separation for aerosol sampling operations.

The cyclone performance is described by use of two parameters, particle collection efficiency defined as the fraction of solids separated and pressure drop. Therefore most attention concerning to cyclone separators has been paid to increase the collection efficiency and to reduce the pressure drop.

The literature shows that a noticeable number of theoretical, numerical and experimental investigations have been carried out on the cyclone separators in the last few decades. Soo[1] conducted a theoretical analysis on the gas flow field, dust dispersion and dust collection in a cyclone separator.

However, during the past years, the application of numerical method for the calculation of the gas flow field in the cyclone separators is becoming more popular. Assuming axisymmetric flow, Ayers et al.[2] and Zhou et al.[3] performed one of the first numerical calculations of gas flow and particle motion in cyclone separators. Zhou and Soo[4] employed the standard k-ε turbulence model to model flow in cyclones. Boysan et al.[5] showed that the standard k-ε turbulence model is inadequate to simulate swirling flows because it assumes the isotropic turbulence, while the flow in cyclone has anisotropic turbulence. As more recent work on the modeling of cyclonic flow, Dyakowski and Williams[6] employed a modified k-ε turbulence model. Pant et al.[7] and Wang et al.[8] used Reynolds Stress model. They showed the superiority of the RSM over k-ε model. Nevertheless, due to high computational cost of RSM, in this study, another common anisotropic turbulence model, the Algebraic Stress Model (ASM), is employed to model the Reynolds stress components.

The experimental investigations on cyclone separators have been developed by a number of contributors using different methods. Boysan et al.[9] have been measured Radial profiles of axial and tangential velocities using a back scatter LDA system. Zhou and Soo[10] measured the velocity distribution of particles in the center of cyclone using Laser Doppler Velocimeter (LDV). Zhao[11] performed an experimental study to compare main flow parameters including tangential velocity, axial velocity and static pressure distribution in two different cyclone separators with conventional and symmetrical inlet geometries.

Apart from many investigations, there are some inherent limitations with traditional dry cyclone separators, such as low collection efficiency of fine particles. Generally, finer particles less than about 3μm can only be removed using some additional methods; such as injecting droplets[12]. Calvert[13] presented the first 1D model to simulate inertial impaction mechanism of droplet-particle. Using the droplet injection, Krames and Buttner[14] conducted an experimental investigation and found that the wet cyclones have better particle removal performance than conventional dry cyclones.

The aim of this research is the examination of the separation performance of a high efficiency dry cyclone separator. An auxiliary system is also employed to improve collection efficiency of dry cyclone separator. This system includes the injection of scrubbing liquid

droplets into the cyclone separator chamber. Finally, the collection efficiency is compared between traditional dry cyclone separator and improved wet cyclone.

2 MATHEMATICAL FORMULATION

In this study, mathematical formulation of a cyclone separator includes the gas phase governing equations, the dispersed Phase tracking model, the model of droplet catching particles and droplet evaporation model.

2.1 Gas Phase Governing Equations

As a conventional approach of modeling the gas flow in a cyclone separator, it is assumed that flow is incompressible, steady and axisymmetric. The governing equations of gas phase are expressed based on conservation of mass and momentum. These equations are given in cylindrical coordinates (x,r,θ), as follow :

$$\begin{cases} x: & \frac{\partial}{\partial x}(uu)+\frac{1}{r}\frac{\partial}{\partial r}(rvu)= \\ & -\frac{1}{\rho}\frac{\partial p}{\partial x}+\nu\left\{\frac{1}{r}\frac{\partial}{\partial r}(r\frac{\partial u}{\partial r})+\frac{\partial^2 u}{\partial x^2}\right\}-\frac{\partial}{\partial x}\left(\overline{u'u'}\right)-\frac{1}{r}\frac{\partial}{\partial r}(r\overline{v'u'}) \\ r: & \frac{\partial}{\partial x}(uv)+\frac{1}{r}\frac{\partial}{\partial r}(rvv)-\frac{w^2}{r}= \\ & -\frac{1}{\rho}\frac{\partial p}{\partial r}+\nu\left\{\frac{\partial^2 v}{\partial x^2}+\frac{1}{r}\frac{\partial}{\partial r}(r\frac{\partial v}{\partial r})-\frac{v}{r^2}\right\}-\frac{\partial}{\partial x}\left(\overline{u'v'}\right)-\frac{1}{r}\frac{\partial}{\partial r}(r\overline{v'v'})+\frac{1}{r}\overline{w'w'} \\ \theta: & \frac{\partial}{\partial x}(uw)+\frac{1}{r}\frac{\partial}{\partial r}(rvw)+\frac{vw}{r}= \\ & \nu\left\{\frac{\partial^2 w}{\partial x^2}+\frac{1}{r}\frac{\partial}{\partial r}(r\frac{\partial w}{\partial r})-\frac{w}{r^2}\right\}-\frac{\partial}{\partial x}\left(\overline{u'w'}\right)-\frac{1}{r}\frac{\partial}{\partial r}(r\overline{v'w'})-\frac{1}{r}\overline{v'w'} \end{cases} \quad (1)$$

Where ρ is the gas density, p is the static pressure, ν is the kinematic viscosity of gas and u,v,w are axial, radial and tangential velocities, respectively.

Taking into consideration the anisotropic flow in cyclone, the Reynolds stress components ($\overline{u_i'u_j'}$) are calculated from an Algebraic Stress model[15]. A usual wall-function approach is adopted to model the near-wall region of the flow.

2.2 Dispersed Phase Governing Equations

A Lagrangian approach is employed to predict the trajectories of each group of dispersed phase (particles and droplets) in cyclone chamber. The time-dependent differential equations of motion of dispersed phase are integrated by a semi-analytic method[16]. The Lagrangian model uses a stochastic method to simulate the turbulent velocity fluctuations of the fluid at particle/droplet location. The effect of velocity fluctuations on separation efficiency is studied by making use of instantaneous fluctuating velocities in the calculation of discrete phase trajectories, instead of the mean velocities.

Some of basic assumption of Lagrangian model can be expressed as:

1- In the mentioned Lagrangian approach, the trajectories of dispersed phase are computed in a known fluid flow. In other words; the influence of particles/droplets on the fluid flow is neglected.
2- Particles/droplets are treated as small spheres.

3- There is no interaction between particles also the break up and agglomeration of droplets is neglected.
4- No force applied on droplet due to the particle adheres to droplet

A particle or droplet motion in gas flow field influenced by external forces include gravity and gas-particle/droplet drag and other forces such as Saffman, force Basset force and etc. are not considered. Thus the equation of motion of particle/droplet in the isothermal gas phase can be expressed as:

$$\begin{cases} \dfrac{du_{l/p}}{dt} = -g - \dfrac{3}{4}\dfrac{\mu}{\rho_{l/p} D_{l/p}^2} C_D \,\mathrm{Re}(u_{l/p} - u - u') \\ \dfrac{dv_{l/p}}{dt} = \dfrac{w_{l/p}^2}{r_{l/p}} - \dfrac{3}{4}\dfrac{\mu}{\rho_{l/p} D_{l/p}^2} C_D \,\mathrm{Re}(v_{l/p} - v - v') \\ \dfrac{dw_{l/p}}{dt} = \dfrac{v_{l/p} w_{l/p}}{r_{l/p}} - \dfrac{3}{4}\dfrac{\mu}{\rho_{l/p} D_{l/p}^2} C_D \,\mathrm{Re}(w_{l/p} - w - w') \end{cases} \quad (2)$$

Where u',v',w' are fluctuating components of velocity field, μ is dynamic viscosity of gas and $D_{l/p}$ is droplet or particle diameter and $u_{l/p}$, $v_{l/p}$, $w_{l/p}$ are axial, radial and tangential velocity of liquid droplet or dust particles, respectively. The drag force per unit mass of dispersed phase can be stated as:

$$F_D = \frac{3}{4}\frac{\mu}{\rho_{l/p} D^2} C_D \,\mathrm{Re}(w_{l/p} - w - w') \quad (3)$$

Which the drag coefficient C_D is a function of particle/droplet Reynolds Number:

$$C_D = \begin{cases} \dfrac{24}{\mathrm{Re}} & ,\mathrm{Re} < 0.1 \\ 3.690 + \dfrac{22.73}{\mathrm{Re}} + \dfrac{0.0903}{\mathrm{Re}^2} & ,\mathrm{Re} < 1.0 \\ 1.222 + \dfrac{29.17}{\mathrm{Re}} - \dfrac{3.889}{\mathrm{Re}^2} & ,\mathrm{Re} < 10.0 \\ 0.617 + \dfrac{46.50}{\mathrm{Re}} - \dfrac{116.7}{\mathrm{Re}^2} & ,\mathrm{Re} < 100.0 \\ 0.364 + \dfrac{98.33}{\mathrm{Re}} - \dfrac{2778}{\mathrm{Re}^2} & ,\mathrm{Re} > 100.0 \end{cases} \quad (4)$$

Where the particle/drop. Reynolds number, Re, is related to relative velocity, V_{rel}, as follow:

$$\begin{cases} \mathrm{Re} = \dfrac{\rho_g D_{l/p} V_{rel}}{\mu_g} \\ V_{rel} = \sqrt{(u_{l/p} - u - u')^2 + (v_{l/p} - v - v')^2 + (w_{l/p} - w - w')^2} \end{cases} \quad (5)$$

2.3 Droplet catching particles model

The droplet catching mechanisms include inertial impaction, interception, and Brownian diffusion. In the cyclone separators the target particles are almost greater than 1μm, then impaction is the primary ones [17].

The Stokes number, Stk, is a non-dimensional parameter describing the particle collection efficiency due to impaction of the particles to droplets. Shi et al. [18] showed that impaction catching efficiency obtained by experiment is lower than theoretical calculations, thus a correction factor k (k=0.8) is applied to adjust the impaction catching efficiency.

$$\eta_{imp} = k\left(\frac{Stk}{Stk+0.35}\right)^2 \tag{6}$$

Where Stk, the Stokes number, is a function of the particle density, ρ_p, gas viscosity, μ, particle-droplet relative velocity, $\left|\vec{u}_D - \vec{u}_p\right|$, droplet diameter, D_{Drop}, and particle diameter, d_p, as below:

$$Stk = \frac{\rho_P d_P^2 \left|\vec{u}_D - \vec{u}_p\right|}{18\mu D_{Drop}} \tag{7}$$

Lim et al.[17] reported the impaction collection efficiency of single droplet as a linear piecewise function of Stokes Number, The following equations describe it:

$$\begin{cases} \eta_{imp} = 0.6(Stk) & Stk \le 1.0 \\ \eta_{imp} = 0.11(Stk) + 0.49 & 1.0 < Stk \le 3.0 \\ \eta_{imp} = 0.02(Stk) + 0.79 & 0.3 < Stk \end{cases} \tag{8}$$

Applying correction factor:

$$\begin{cases} \eta_{imp} = 0.48(Stk) & Stk \le 1.0 \\ \eta_{imp} = 0.088(Stk) + 0.391 & 1.0 < Stk \le 3.0 \\ \eta_{imp} = 0.016(Stk) + 0.632 & 0.3 < Stk \end{cases} \tag{9}$$

2.4 Droplet evaporation rate model

The evaporation rate of single droplet is also governed by local mass transfer coefficient and vapor concentration[19]. These parameters define the flux of droplet vapor into the gas phase:

$$N_i = k_c\left(C_{i,s} - C_{i,\infty}\right) \tag{10}$$

Which N_i is molar molar flux of vapor, k_c is mass transfer coefficient, $C_{i,s}$ is vapor concentration at the droplet surface and $C_{i,\infty}$ is vapor concentration in the bulk gas[19]:

$$\begin{cases} C_{i,s} = \dfrac{p_{sat}\left(T_{Drop}\right)}{RT_p} \\ C_{i,\infty} = \dfrac{\phi P_{sat}\left(T_{Drop}\right)}{RT_\infty} \end{cases} \tag{11}$$

In this equation, $P_{sat}(T_{drop})$ is saturated pressure in droplet temperature, Φ is relatve humidity and T_∞ is ambient temperature.

Generally, droplet evaporation rate can be either diffusion-controlled or dynamic mixing-controlled or both. Since, the flow is turbulent in cyclone separators, mass transfer coefficient can be expressed as[20]:

$$k_c = D_{i,m}\left(2.0 + 0.6\,\mathrm{Re}_d^{1/2}\,Sc^{1/3}\right)\Big/ D_{Drop} = Sh \times D_{i,m} / D_{Drop} \tag{12}$$

Where Sh is Sherwood number, Sc is Schmidt number and $D_{i,m}$ is vapor diffusivity to gas.

Finally, the diameter of droplet is obtained

$$D_{Drop}(t+\Delta t) = \left\{ D_{Drop}^3(t) - \left(\frac{6}{\rho_{water}} N_i D_{Drop}^2(t) M_{water} \Delta t \right) \right\}^{\frac{1}{3}} \tag{13}$$

3 COMPUTATIONAL PROCEDURE

The Eulerian partial differential equations of the gas phase conservation of mass and momentum are discretized by use of control-volume based method of Patankar[21] in the computational domain. All discretized equations are solved by a line-by-line iterative procedure. The general discretized equation can be expressed as algebraic equation, as follow:

$$a_P \phi_P = \sum_{nb} a_{nb} \phi_{nb} + S \tag{14}$$

Where a_P, a_{nb} are coefficients; subscript P indicates the control volume center on which the dependent variable is computed, ϕ can be V_r, V_x, P, k or ε; subscript nb refers to the nearest neighboring control volume centers and S represents the linearized source terms.

Due to the elliptic nature of conservation equations, all boundary conditions concerning to flow field must be defined. In this study, both geometry and boundary conditions of cyclone separator are axisymmetric about the horizontal axis. Therefore, the problem can be reduced by considering only a longitudinal section of the cyclone separator as the computational domain and applying symmetry boundary condition along the cyclone axis.

The geometry of high performance cyclone separator is selected according to experimental investigation were presented by Ayers [2]. The geometrical configuration and dimensions of the cyclone to be studied are shown in Fig. 1, where

$$D_c = 0.29\ \mathrm{m} \quad L_c = 0.308\ \mathrm{m} \quad L_{cyclone} = 0.82\ \mathrm{m} \quad D_b = 0.074\ \mathrm{m} \quad D_e = 0.103\ \mathrm{m} \tag{15}$$

The inlet conditions are defined by uniform distribution of inward radial velocity, according to air volumetric flow rate $Q = 0.08\,m^3/s$, and the uniform tangential velocity $w_{in} = 20\,m/s$ [2]. The inlet kinetic energy and dissipation rate being given by [22]:

$$k = 0.005 U_{in}^2 \quad , \varepsilon = C_\mu k^{1/2} / 0.003R \tag{14}$$

At the outlet boundary, vortex finder pressure outlet, and symmetry axis, zero gradient conditions are applied. The no slip condition is applied on the all cyclone walls.

A line by line iterative method is used to solve the set of algebraic equations, starting from the specified initial conditions. The convergence criterion is determined by the requirement that the maximum value of the normalized residuals of each equation must be less than 1.5×10^{-4}. The converged flow field is obtained after about 25000 iterations. To secure the convergence of iteration procedure, the under-relaxation factors are used for velocity, pressure, turbulent kinetic energy and dissipation rate equations. The range of under

relaxation factors are set to 0.8 for turbulent kinetic energy and dissipation rate, 0.2 for pressure and 0.45 for velocity equations.

Once a converged flow is obtained, the equations for discrete phase can be solved. Using a Lagrangain approach all particles and droplets are tracked in cyclone chamber. In present study, the trajectories of discrete phases are obtained in three stages. In the first stage, the solid particles are divided into 9 classes according to particles diameter and its diameters vary between 1-9 microns. The solid particles are injected into cyclone chamber by uniform spatial distribution at tangential inlet. The separating efficiency and trajectories of particles in dry cyclone separator are employed to define best droplet injection conditions, such as droplet diameter, nozzle angle and injection velocity. In the second stage, the water droplets are injected into cyclone chamber. The droplet nozzle located on the vortex finder. The nozzle angle varies between -45 to +10 and injection velocity changed between 5 to 100 m/sec. the most favorable conditions of droplet injection can be expressed as minimum evaporation of droplets and maximum displacement in cyclone chamber. The best conditions of droplet injection are chosen in this step. As a final stage, droplets are injected into cyclone chamber to improve the collection efficiency of fine particles.

The computational domain of the cyclone separator is divided in 50×39 grid (axial×radial) in a uniform distribution. A grid dependence study is performed to find out the appropriate size of the grid to gain the grid independent results. The grid is varied from (50×39), (75×59), (100×81), (150×121) to (200×162) for a typical set of operating conditions. Comparing axial and tangential velocities at a specified place in cyclone disclosed that increasing grid number from (150×121) to (200×162) made very small variation on the flow field behavior. Therefore, a grid size of (150×121) is chosen for all following computations.

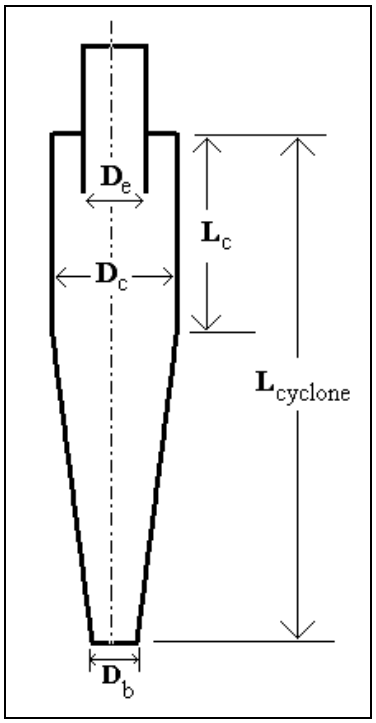

Fig. 1. The geometry of high efficiency cyclone separator

4 RESULTS AND DISCUSSION

To allow comparison with experimental measurement, all boundary conditions corresponding to the cyclone separator of Ayers[2] are incorporated in computational procedure. Figure 1 compares the radial profiles of axial and tangential velocity with measurements at a longitudinal section of cyclone separator. It reveals that the numerical scheme can fairly simulate the flow field quantities and numerical predictions are in good agreement with the measurements.

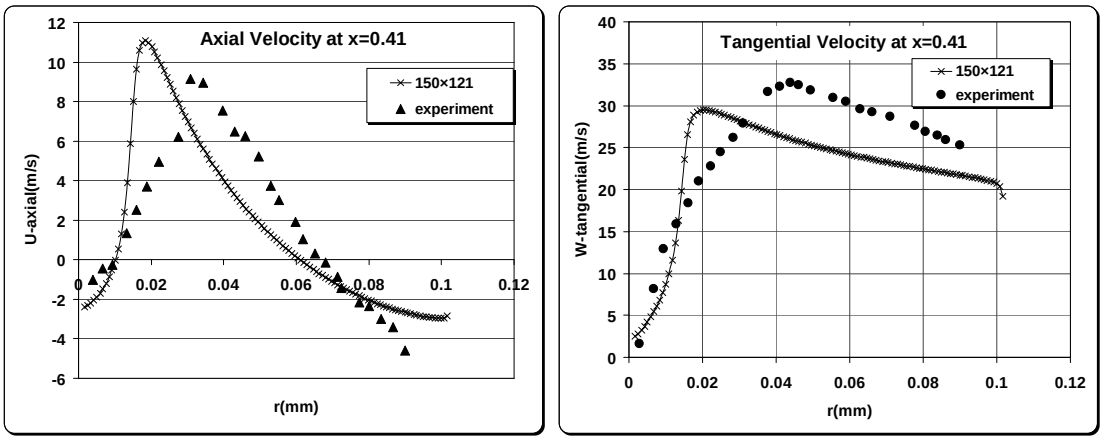

Figure 2: Comparison of computational axial and tangential velocities with experimental results at x=0.41 m

Figure 3 determines how different sizes of dust particles, with size of 1 to 9 μm move in the cyclone separator. It can be seen that the centrifugal force throws the particles to the cylindrical walls. After that, the gas flow drag moves these particles down. The larger particles collide with the wall and change their path to the down of cyclone chamber. This process continues till the particles hit the bottom of the cyclone and collect there. Some other particles exit from the exhaust tube or remain suspended for a relatively long time without being deposited on the surface.

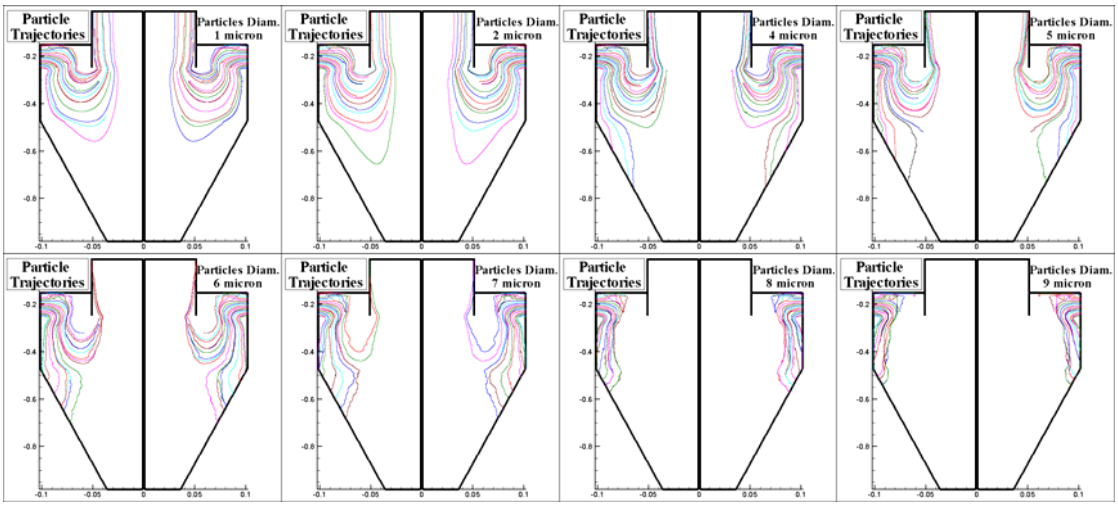

Figure 3: Trajectories of dust particles little than 10 micron in the cyclone chamber

It is clear from the figure that the influence of centrifugal forces on particles <3 μm is negligible. All of these particles follow the gas streamlines and do not collide with the walls during leaving the cyclone. Hence, dust collection efficiency is very low for particles little than 3 μm. Furthermore, it can be seen that the dust collection efficiency increases with an increase in particle size, however; considering fluctuations decreases the collection efficiency. They make some particles larger than 8 μm remain suspended and collection efficiency can not be reached to 100%.

Figure 4 presents the influence of turbulence on the separation efficiency of cyclone separator. It can be seen that considering velocity fluctuations can decrease the separation efficiency. The reason for this is that the small vortices in a fluctuating velocity field make some particles remain suspended and not collected.

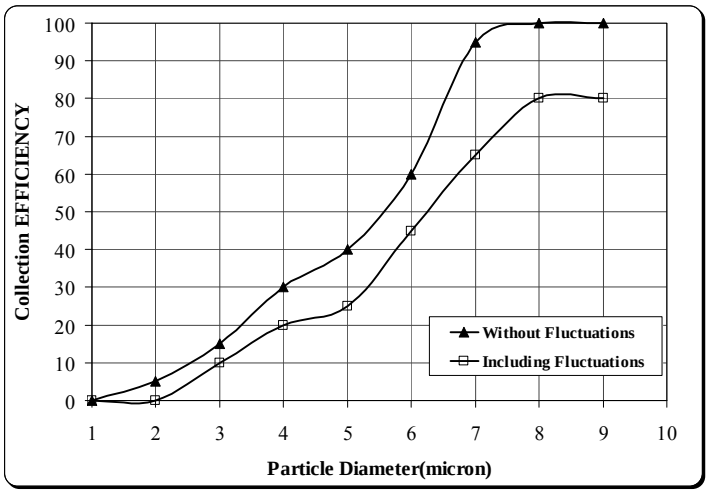

Figure 4: The influence of velocity fluctuations on the collection efficiency of cyclone separator

As an approach to improve the separation efficiency of dry cyclone separator, the water droplets are injected into cyclone chamber. Figure 5 presents the effect of droplet diameters and nozzle angle on the droplet paths in cyclone chamber. The injection velocity is set to 100m/s

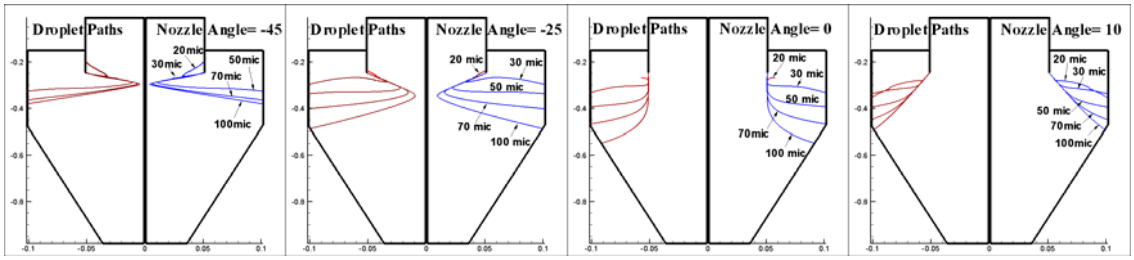

Figure 5: Effect of droplet diameter on the droplet trajectories in cyclone chamber

The comparison between different nozzle angles indicates that in the range of nozzle angle between -45 to zero the droplets ≤ 20μm, evaporate completely before hitting the wall of cyclone separator. This is due to the small droplets fall into vortices and remain till evaporate completely. As well, this figure shows that at every nozzle angles, large droplets (100 μm) pass a longer distance before hitting the wall. In other words; large droplets can collect more particles for a typical set of operating conditions. Thus, the droplet diameter of 100 μm is chosen to collect fine particles.

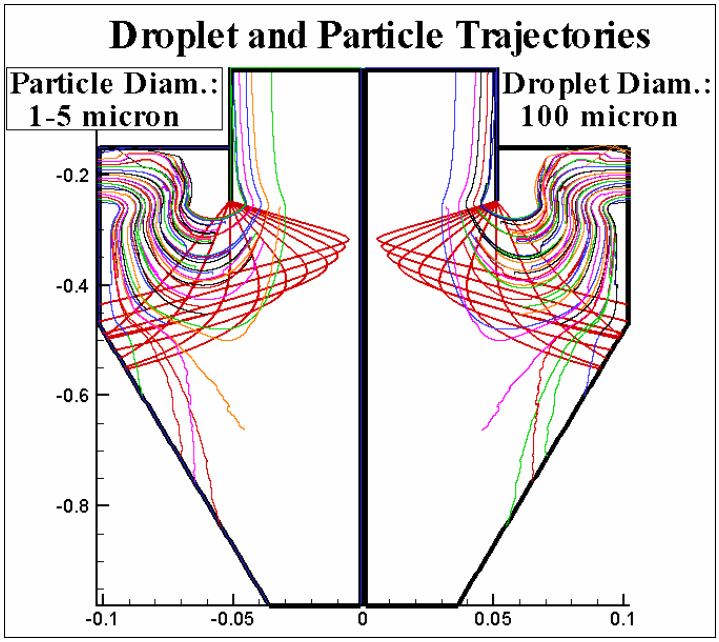

Figure 6: Droplet and Particle trajectories in the high efficiency wet cyclone separator

Figure 6 displays the trajectories of particles < 5μm and the injected droplets in cyclone chamber. The nozzle angle vary between -45 to +10 and injection velocity is set to 100 m/s. As mentioned previously, the droplet catching efficiency is calculated based on impaction efficiency and Stokes number. An impaction with droplet catching efficiency> 50%, leads to collect dust particle. Figure 7 shows the collection efficiency of dry and wet cyclone separator. It can be seen that injection of liquid droplet can enhance separation efficiency of cyclone separator, especially for particles smaller than 5 μm.

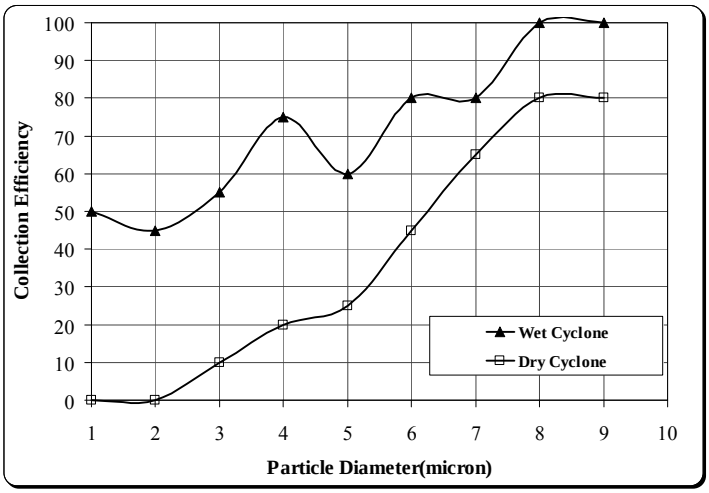

Figure 7: The effect of droplet injection on the collection efficiency of cyclone separator

5 CONCLISIONS

In this investigation, the effect of droplet injection on the separation efficiency of a cyclone separator is presented. A Lagrangian approach is used to track the dust particles and water droplets in cyclone chamber. Droplets are injected into laden gas flow of cyclone to enhance the collection efficiency. The impaction is considered as the primary catching dust mechanism. The numerical procedure is validated by comparing the numerical results of axial and tangential velocities with experimental measurements at a longitudinal section of cyclone. Computational results indicate that considering fluctuation velocities would decrease separation efficiency of cyclone, while the injection of liquid droplet can enhance the cyclone performance, especially for fine particles. Also, the calculations reveal that droplet size has strongly effect on the droplet path motion.

REFERENCES

[1] S. L. Soo, Particulates and Continuum Multiphase Fluid Dynamics, Hemisphere, New York, p. 254, (1989).

[2] W. H. Ayers, F. Boysan, J. Swithernback and C. R. Ewan, Theoretical modeling of cyclone performance, Filtration and Separation: 39-43 (1985).

[3] L. X. Zhou, R. X. Li, T. Q. Qiu, J. S. Liu and X. Q. Huang: Proceedings of Second World Congress, Particle Tech., 72 (1990).

[4] L. X. Zhou, S.L. Soo, Gas–solid flow and collection of solids in a cyclone separator, Powder Technol., 63 (1) 45–53 (1990).

[5] F. BOYSAN, W.H. AYER, J. A. SWITHENBANK, “Fundamental mathematical-modeling approach to cyclone design”, Transaction of Institute Chemical Engineers, 60 (1982) 222-230.

[6] T. Dyakowski, R.A. Williams, Modeling turbulent flow within a small-diameter hydrocyclone, Chem. Engng Sci., 48(6), 1143-1152 (1993).

[7] K. Pant, C. T. Crowe, P. Irving, On the design of miniature cyclone for the collection of bioaerosols, Powder Technology, 125, 260-265 (2002).

[8] B. Wang, D.L. Xu, K.W. Chu, A.B. Yu, Numerical study of gas solid flow in a cyclone separator, Applied Mathematical Modeling, 30, 1326-1342 (2006).

[9] F. Boysan, B. C. R. Ewan, J. Swithenbank, W. H. Ayres, Experimental and theoretical studies of cyclone separator aerodynamics, IChemE. Symp. Series, No 69: 305-320 (1983).

[10] Zhou, L. X. and S. L. Soo, Gas-solid flow and collection of solids in a cyclone separator, Powder Technology 63(1): 45-53(1990).

[11] B. Zhao, Experimental investigation of flow patterns in cyclones with conventional and symmetrical inlet geometries, Chem Eng Technol, 28(9): 969–972 (2005).

[12] K.-S. Yang and H. Yoshida, Effect of mist injection position on particle separation performance of cyclone scrubber, Separation Purification Technology **37**, pp. 221–230 (2004).

[13] S. Calvert, Venturi and other atomizing scrubbers efficiency and pressure drop., A.I.Ch.E. Journal 16 (3), pp. 3962–3966, (1970).

[14] J. Krames, H. Buttner, The cyclone scrubber—a high efficiency wet separator, Chem. Eng. Technol. 17, pp. 73–80, (1994).

[15] Zh. Jian, N. Sen and Zh. Lixing, a new algebraic stress model for simulating strongly swirling flows, Numerical heat transfer, Part B, 22, p. 49, (1992).

[16] F. Boysanand J. Swithenbank, Spray evaporation in recirculating flow, International Symposium on Combustion, (1978).

[17] K.S. Lim, S.H. Lee, H.S. Park, Prediction For Particle Removal Efficiency of a Reverse Jet Scrubber, Journal of aerosol science, 37, pp. 1826-1839, 2006

[18] J. Shi, J.D. Wang, G.Z.Yu, Chemical Engineering Handbook, Chemical Industry Press, Beijing, (1996)

[19] Fluent user guide, version 6.3.26, (2005).

[20] D. Basmadjian, Mass Transfer principles and applications, CRC Press, (2004)

[21] S.V. Patankar, Numerical Heat Transfer and Fluid Flow, McGraw-Hill, (1980).

[22] J. C. S. Lai, C. Y. Yang, Numerical simulation of turbulence suppression comparisons of the performance of four k-ε turbulence models, Int. J. Heat and Fluid Flow, 18 No. 6 (1997).